RSC Advances

Journal Name

COMMUNICATION

Bis(phosphine oxide)/ triphenylamine based material for solution-processed blue electrofluorescent and green electrophosphorescent devices

Wei Jiang*, Peng Cui, Xinxin Ban, Yueming Sun*

**A novel material TPA-BPhPO with the photoluminescence quantum yield of 68% and the triplet energy of 2.48 eV has been designed and synthesized. High external quantum efficiencies of 1.41% and 9.3% were achieved in solution-processed blue electrofluorescent and green electrophosphorescent devices, respectively.**

Solution-processed organic lighting-emitting diodes (OLEDs) are attracting more and more attention due to simple and low cost fabrication processes.[1-5] From the perspective of the flexible application, solution-processed white OLEDs with high power efficiencies are required. In pursuing efficient solution-processed white OLEDs, recent reports are almost based on phosphorescent emitters that have an inherently higher efficiency in converting both singlet and triplet excitons into photons than their fluorescent counterparts.[6-15] However, one of the serious weaknesses of this system is that fast chemical degradation processes usually occur in blue phosphorescent emitters (such as FIrpic and FIr6) during device operation.[16, 17] Recently, fluorescent/phosphorescent hybrid structure devices have been developed to solve this problem.[18-20] In this strategy, the device harvests 100% internal quantum efficiency by utilizing the 25% singlet excitons formed from charge recombination in blue-emitting fluorescent host material while transferring the remaining 75% triplet excitons to green, orange or red phosphorescent emitter. In order to realize this point, the multifunctional blue fluorophors should be developed to be used as blue emitters and host materials for phosphorescent dopants simultaneously, which are demanded to possess both high fluorescence quantum efficiency and high triplet energy. Up to now, many efficient blue fluorophors such as anthracene[21-23], pyrene[24, 25], fluorene[26-28] and carbazole[29-31] derivatives have been developed with success. However, most successfully developed blue fluorophors are inferior in triplet energy due to their long effective conjugation length and only few reports on efficient blue fluorophors with high triplet energy were found in the literatures. For example, Wong et al reported an efficient bipolar deep-blue emitter CPhBzIm with a high triplet energy (E_T=2.48 eV).[32] Zhang et al reported an ideal sky-blue emitter DADBT with E_T value of 2.38 eV and a high efficiency blue OLEDs with an external quantum efficiency of 5.12% was

achieved.[33] Therefore, there is a strong demand for the development of multifunctional blue fluorophors with high triplet energies.

In this work, we have designed and synthesized a new triphenylamine (TPA)-based blue fluorophor 4'-(diphenylamino)-[1,1'-biphenyl]-3,5-diyl)bis(diphenylphosphine oxide (TPA-BPhPO), containing a bis(diphenylphosphine oxide) unit for the purpose of improving fluorescent quantum yield, due to its strong intramolecular charge transfer character. Diphenylphosphine oxide (PO) is known to be an excellent electron transport material with a high triplet energy[34-37], while TPA is commonly used in hole-transporting and host materials for its excellent hole-transporting property and high triplet energy.[38-41] As a result, TPA-BPhPO is expected to possess bipolar transporting nature and balance the charge fluxes in emitting layer. TPA-type materials usually have high HOMO levels, which are close to the work function of ITO or the widely used hole injection material PEDOT:PSS, thus facilitating the transfer of holes in the devices. Furthermore, TPA-BPhPO possesses a high triplet energy, which is suitable to serve as an appropriate host for green PhOLEDs.
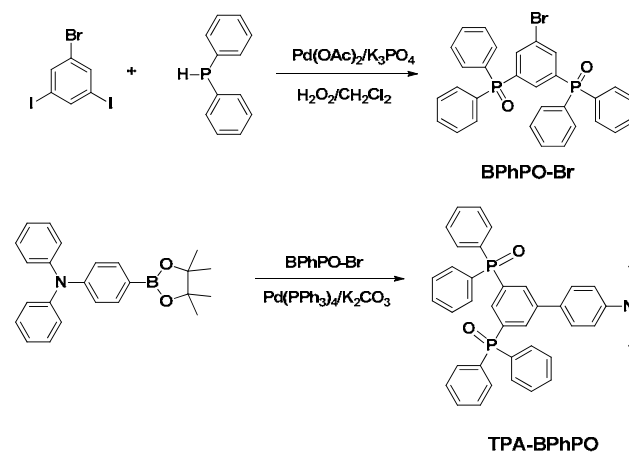
Scheme 1 Synthetic routes toward TPA-BPhPO.

As shown in Scheme 1. TPA-BPhPO can easily be synthesized through a two-step reaction with moderate yield. First, BphPO-Br is synthesized by the C-P coupling reaction between 1-bromo-3,

diiodobenzene and diphenylphosphine and then oxidized with an excess of 30% hydrogen peroxide solution in 50.6% yield. TPA-BPhPO is achieved by the palladium-catalyzed Suzuki coupling reaction of BPhPO-Br with the TPA boronic esters in 65% yield. The final product is purified by silica gel chromatography and further purified by recrystallizaiton from ethyl acetate solvent before device fabrication. The structures of compounds are fully characterized by ^{1}H-NMR, ^{13}C-NMR, mass spectrometry and elemental analysis, as described in the experimental section. The thermal property of TPA-BPhPO is investigated by thermal gravimetric analyses (TGA) and differential scanning calorimetry (DSC). As shown in Fig. S2, TPA-BPhPO exhibits excellent thermal stability with the same decomposition temperature (T_d, 5% weight-loss) of 416 °C, with the glass transition temperature (T_g) of 92 °C. The surface roughness of neat TPA-BPhPO and 8wt% Ir(mppy)$_3$ doped TPA-BPhPO on ITO/PEDOT:PSS is investigated by AFM (Fig. S3). The films are smooth and free of pinholes, with root-mean-square (RMS) values of 0.82 and 0.75 nm, respectively. These results demonstrate that TPA-BPhPO is capable of forming amorphous films and enables the fabrication of devices through solution processing.
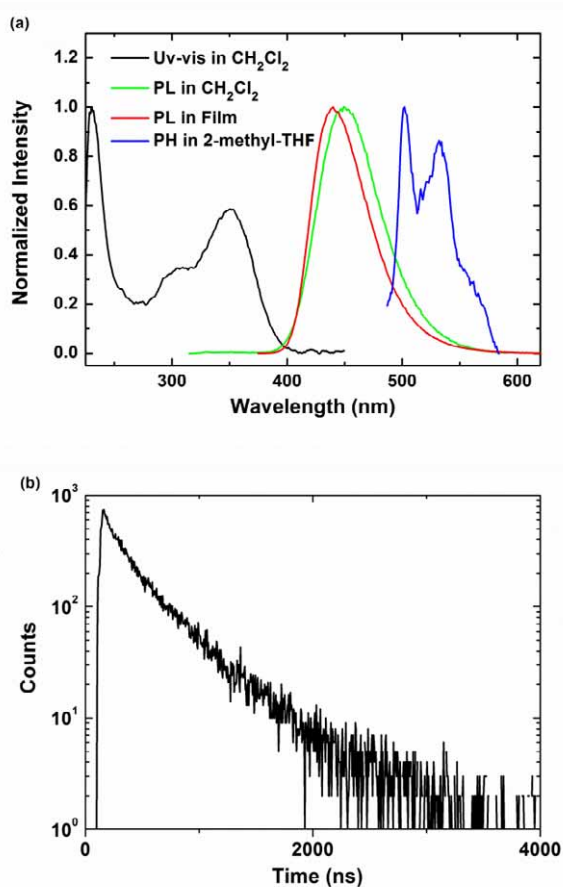

Fig. 1 (a) Absorption spectra of TPA-BPhPO in dichloromethane solution, photoluminescence spectra of TPA-BPhPO in dichloromethane solution and in the film state, and phosphorescent spectra of TPA-BPhPO in 2-methyltetrahydrofuran at 77K; (b) Transient photoluminescence decay curve of 5 wt% Ir(mppy)$_3$-doped TPA-BPhPO film monitored at 520 nm.

The room temperature UV-vis absorption of TPA-BPhPO in CH$_2$Cl$_2$ is investigated. As shown in Fig. 1a, two absorption bands around 306 and 348 nm are observed, which can be attributed to the

n-π* transitions of TPA moiety and intramolecular charge transfer (ICT) transition from the electron-donating triphenylamine to the electron-accepting PO moiety, respectively. The photoluminescence (PL) emission of TPA-BPhPO in dilute CH$_2$Cl$_2$ exhibits peak at 44? nm, while its thin film shows a 10 nm hypsochromic shift with a PL quantum yield of 0.68. The triplet energy of TPA-BPhPO is estimated from the 0-0 transitions in their low-temperature phosphorescent spectra, giving a value of 2.48 eV. The E_T value of TPA-BPhPO is high enough to be used as a host material for the green triplet emitter. To further confirm its exciton confinement property, the transient photoluminescence decays of TPA-BPhPO film doped with 5% Ir(mppy)$_3$ is measured. As shown in Fig. 1b, the Ir(mppy)$_3$-doped film exhibits monoexponential decay curve, which demonstrate that the energy back-transfer from Ir(mppy)$_3$ to TPA-BPhPO is completely suppressed.
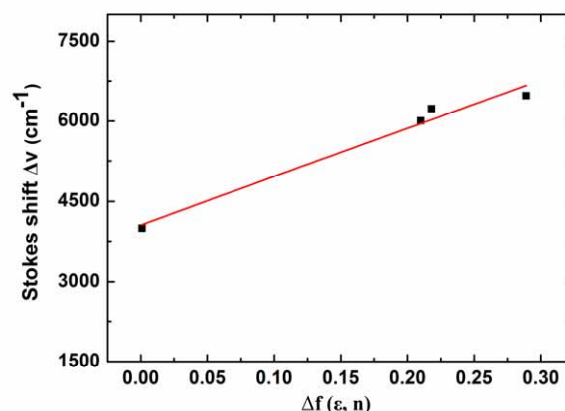

Fig. 2 Lippert-Mataga plot of TPA-BPhPO in various solutions.

To gain more insight fluorescence spectra of TPA-BPhPO is recorded in various solvents with different polarity. As a change of the solvent from n-hexane to acetonitrile, the maximum absorption wavelengths are red-shifted from 347 to 358 nm, while the maximum emission wavelengths are red-shifted from 403 to 466 nm. The large Stokes shift in polar solvents indicates that the excited state is stabilized in more polar solvents, as expected for an ICT. T? obtain more information about the change in the dipole moment upon excitation, we use the Lippert-Mataga equation, which express the Stokes shift as a function of the solvent polarity parameter.[42] Fig.2 shows the linear Lippert-Mataga plots with the slope value of 4020 cm^{-1} for TPA-BPhPO. From the slope of this plot, the difference of the dipole moment between the excited state and the ground state is estimated to be 17.2 D. This large change in dipole moment upon excitation is typical for photoinduced intramolecular CT processes, reflecting the effective electronic communication between the donor TPA unit and the acceptor PO unit.

The electrochemical property of TPA-BPhPO is studied in solution through cyclic voltammetry (CV) using tetrabutylammonium hexafluorophosphate (TBAPF6) as the supporting electrolyte and ferrocene as the internal standard. Fig. 3 shows that TPA-BPhPO has distinct reduction and oxidation behaviors, which indicate their potential in bipolar carrier transport. During the anodic sweeping in CH$_2$Cl$_2$, the CV curve of TPA-BPhPO shows reversible oxidation waves with onset potential of 0.49 V, which arised from its electron-donating TPA unit. On t? basis of the onset potential for oxidation, the highest occupied molecular orbital (HOMO) value of TPA-BPhPO is estimated to be -5.29 eV, which is close to the work function of PEDOT. The we? matched energy levels of TPA-BPhPO with PEDOT can lead to t? reduction of holes injection barrier, thereby facilitating the injection

of positive charge carriers to emitting layer. During the cathodic scan in DMF, TPA-BPhPO shows the reversible reduction processes originating from electron-acceptor PO unit. The LUMO level is thus calculated to be -2.54 eV for TPA-BPhPO.
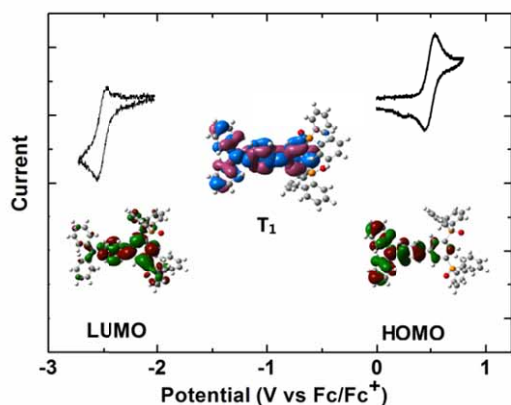

Fig. 3 Cyclic curves of TPA-BPhPO (inset: calculated HOMO and LUMO density maps, and spin-density distribution of T_1 state).

DFT calculation is performed to understand photophysical properties of TPA-BPhPO. The optimized geometry shows that the TPA and bis-PO units are significantly twisted with each other, resulting in a non-planar structure. As shown in Fig. 3, the HOMO is mainly located on the electron-donating TPA moiety, while the LUMO electron density distribution is dispersed over the electron-accepting PO unit and biphenyl core. The separation of HOMO and LUMO is believed to facilitate the hole and electron transporting. To further understand hole and electron-transport properties in these hosts, we performed DFT calculations on the corresponding reorganization energies (λ_+ and λ_-). It could be observed that the value of k+/k- (the calculate ratio of hole- and electron-transfer rate) is 5.80 for TPA-BPhPO, which indicates the bipolar charge-transport property of TPA-BPhPO. It is noteworthy that the HOMO and LUMO of TPA-BBhPO show considerable degree of spatial overlap, indicating a strong ICT interaction and consequently to its high PL quantum yield. Furthermore, the triplet state of TPA-BPhPO is also simulated to obtain the spin-density distributions (SDDs), which indicate the locations of the T_1 excited states. According to the contours of the SDDs, the T_1 states of TPA-BPhPO is mainly located on TPA and biphenyl units. It is noteworthy that the central biphenyl is planar in excited state, while the dihedral angle of the central biphenyl unit is 34° in ground state. As we known, the E_T values of molecules are strongly dependent upon their effective conjugation length in excited state. Thus, compare with high triplet energies of TPA and PO units, TPA-BPhPO shows a decreased E_T value, due to the extent of conjugation between the central phenyl units is increased in excited state.

To assess the utility of TPA-BPhPO as a blue emitter in solution-processed OLEDs, we have fabricated non-doped single-layer (A) and double-layer (B) electrofluorescent devices with the configurations of ITO/PEDOT:PSS/TPA-BPhPO/Cs_2CO_3/Al and ITO/PEDOT:PSS/TPA-BPhPO/TPBi/Cs_2CO_3/Al. In these devices, the conducting polymer PEDOT:PSS is used as the hole injection layer, Cs_2CO_3 is used as the electron-injection layer, TPBi is used as the electron-transporting layers. Fig. S4 presents the current density-voltage-luminance characteristics, while Fig.4 exhibits the curves of luminance efficiency versus current density and the electroluminescence (EL) spectra. Single-layer device A exhibits a turn-on voltage of 3.8 V, the maximum luminance

efficiency (*LE*) and external quantum efficiency (*EQE*) of 0.75 cd/A and 0.91%, respectively, while double-layer device B shows more better performance with a turn-on voltage of 4.0 V, the maximum *LE* of 1.2 cd/A and the maximum *EQE* of 1.41 %. Additional, both device A and B show deep blue emissions with the same maximum peak at 440 nm and corresponding CIE coordinates of (0.16, 0.10) and (0.16, 0.11). It is noteworthy that the EL spectra of devices are similar to its PL spectrum, indicating the efficient suppression of the excimer during the device operation.

Furthermore, single-layer (C) and double-layer (D) electrophosphorescent devices via solution process were fabricated by doping Ir(mppy)$_3$ in the emitting layer with the configurations of ITO/PEDOT:PSS/TPA-BPhPO: Ir(mppy)$_3$ (8 wt%)/Cs_2CO_3/Al and ITO/PEDOT:PSS/TPA-BPhPO: Ir(mppy)$_3$ (8 wt%)/TPBi/Cs_2CO_3/Al. As shown in Fig. S4 and Fig. 4, device C exhibits a turn-on voltage of 3.6 V, the maximum *LE* of 17.4 cd/A, and the maximum *EQE* of 5.1%. After the insertion of the TPBi layer, device D shows largely improved performance with a turn-on voltage of 3.5 V, the maximum *LE* of 32.6 cd/A and the maximum *EQE* of 9.3%. The electrophosphorescent spectra of device C and D are identical with the CIE coordinates of (0.32, 0.60) and (0.31, 0.61), corresponding to the emission from Ir(mppy)$_3$. No additional emission from host is observed, indicating completely energy transfer between the host and guest materials. The low turn-on voltage of devices may be attributed to the high HOMO energy level of TPA-BPhPO, which is effective to improve the injection and transport of holes. Moreover, these devices show small degree efficiency roll-off at higher brightness, which can be ascribed to the bipolar transporting property of TPA-BPhPO. The blue electrofluorescent and green electrophosphorescent devices performance are comparable with the high values reported for solution-processed non-doped deep blue OLEDs and green PhOLEDs.[43-47]
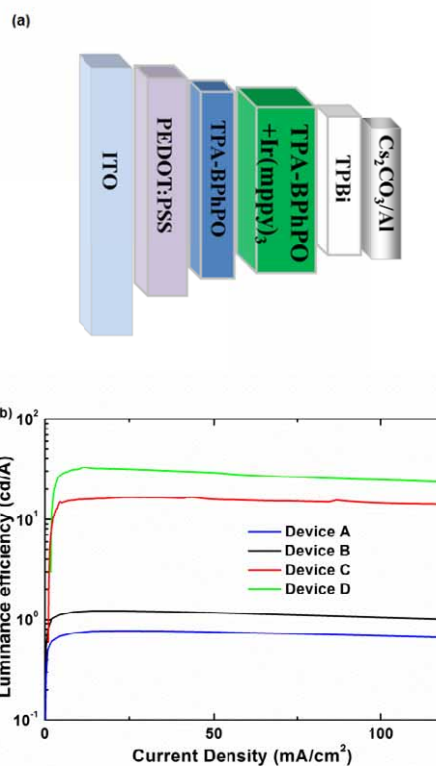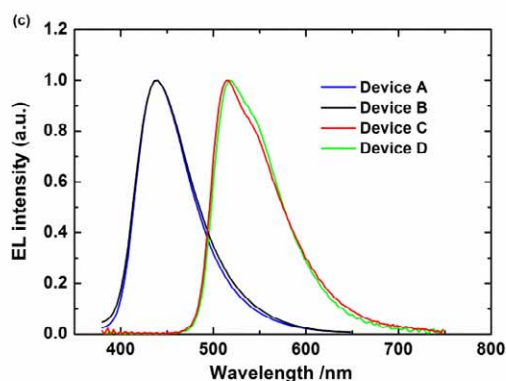
Fig. 4 (a) Schematic diagram of the devices; (b) Luminance efficiency versus current density plots; (c) EL spectra for the devices.

In summary, a novel material TPA-BPhPO for solution-processed blue electrofluorescent and green electrophosphorescent devices has been designed and synthesized. TPA-BPhPO shows the high triplet energy of 2.54 eV and the good PL quantum yield of 68% at the same time. The resulting solution-processed blue electrofluorescent device shows a turn-on voltage of 4.0 V and the maximum *EQE* value of 1.41%, while the solution-processed green electrophosphorescent device shows a lower turn-on voltage of 3.5 V and the maximum *EQE* value of 9.3%.

Notes and references

School of Chemistry and Chemical Engineering, Southeast University, Nanjing, Jiangsu 211189, PR. E-mail: jiangw@seu.edu.cn (W. Jiang); sun@seu.edu.cn (YM. Sun); Fax: +86 25 86792637; Tel: +86 25 52090621

† Footnotes should appear here. These might include comments relevant to but not central to the matter under discussion, limited experimental and spectral data, and crystallographic data.

Electronic Supplementary Information (ESI) available: Synthetic procedures, NMR and device characterizations, See DOI: 10.1039/c000000x/

1 H. Sasabe, N. Toyota, H. Nakanishi, T. Ishizaka, Y. J. Pu and J. Kido, *Adv. Mater.*, 2012, **24**, 3212.

2 L. Duan, L. D. Hou, T. W. Lee, J. Qiao, D. Q. Zhang, G. F. Dong, L. D. Wang and Y. Qiu, *J. Mater. Chem.*, 2010, **20**, 6392.

3 K. S. Yook and J. Y. Lee, *Adv. Mater.*, 2014, **26**, 4218.

4 C. M. Zhong, C. H. Duan, F. Huang, H. B. Wu and Y. Cao, *Chem. Mater.*, 2011, **23**, 326.

5 F. So, B. Krummacher, M. K. Mathai, D. Poplavskyy, S. A. Choulis and V.-E. Choong, *J. Appl. Phys.*, 2007, **102**, 091101.

6 M. A. Baldo, D. F. O'Brien, Y. You, A. Shoustikov, S. Sibley, M. E. Thompson and S.R. Forrest, *Nature*, 1998, **395**, 151.

7 J. Ding, B. Zhang, J. LÜ, Z. Xie, L. Wang, X. Jing and F. Wang, *Adv. Mater.*, 2009, **21**, 4983.

8 X. Wang, S. Wang, Z. Ma, J. Ding, L. Wang, X. Jing and F. Wang, *Adv. Funct. Mater.*, 2014, **24**, 3413.

9 L. D. Hou, L. Duan, J. Qiao, W. Li, D. Q. Zhang and Y. Qiu, *Appl. Phys. Lett.*, 2008, **92**, 263301.

10 W. Tian, Q. Qi, B. Song, C. Yi, W. Jiang, X. Cui, W. Shen, B. Huang and Y. Sun, *J. Mater. Chem. C.*, 2015, **3**, 981.

11 W. Tian, C. Yi, B. Song, Q. Qi, W. Jiang, Y. Zheng, Z. Qi and Y. Sun, *J. Mater. Chem. C.*, 2014, **2**, 1104.

12 Y. Lee, Y. Chang, M. Lee, P. Chiang, C. Chen and C. Chen, *J. Mater. Chem. C.*, 2014, **2**, 382.

13 B. Huang, W. Jiang, J. Tang, X. Ban, R. Zhu, H. Xu, W. Yang and Y. Sun, *Dyes. Pigm.*, 2014, **101**, 9.

14 Y. S. Yook and J. Y. Lee, *Adv. Mater.*, 2014, **26**, 4218.

15 Y. Tao, C. Yang and J. Qin, *Chem. Soc. Rev.*, 2011, **40**, 2943.

16 I. Moras, S. Scholz, B. Lussem and K. Leo, *Org. Electron.*, 2011, **12**, 341.

17 R. Seifert, I. Moras, S. Scholz, M. Gather, B. Lussem and K. Leo, *Org. Electron.*, 2013, **14**, 115.

18 J. Wang, X. Xu, Y. Tian, C. Yao, R. Liu and L. Li, *J. Mater. Chem C.*, 2015, **3**, 2856.

19 M. Kondakova, J. Deaton, T. Pawlik, D. Giesen, D. Kondakov, R. Young, T. Royster, D. Comfort and J. Shore, *J. Appl. Phys.*, 2010, **107**, 014515.

20 X. Liu, C. Zheng, M. Lo, J. Xiao, C. Lee, M. Fung and X. Zhang, *Chem. Commun.*, 2014, **50**, 2027.

21 S. K. Kim, B. Yang, Y. Ma, J. H. Lee and J. W. Park, *J. Mater. Chem.*, 2008, **18**, 3376.

22 S. K. Kim, B. Yang, Y. I. Park, Y. Ma, J. Y. Lee, H. J. Kim and J. W. Park, *Org. Electron.*, 2009, **10**, 822.

23 K. R. Wee, W. S. Han, J. E. Kim, A. L. Kim, S. Kwon and S. O. Kang, *J. Mater. Chem.*, 2011, **21**, 1115.

24 K. C. Wu, P. J. Ku, C. S. Lin, H. T. Shih, F. I. Wu, M. J. Huang, J. J. Lin, I. C. Chen and C. H. Cheng, *Adv. Funct. Mater.*, 2008, **18**, 67.

25 K. L. Chan, J. P. F. Lim, X. Yang, A. Dodabalapur, G. E. Jabbour and A. Sellinger, *Chem. Commun.*, 2012, **48**, 5106.

26 Z. Jiang, Z. Liu, C. Yang, C. Zhong, J. Qin, G. Yu and Y. Liu, *Adv. Funct. Mater.*, 2009, **19**, 3987.

27 C. C. Wu, Y. T. Lin, K. T. Wong, R. T. Chen and Y. Y. Chien, *Adv. Mater.*, 2004, **16**, 61.

28 X. Ban, H. Xu, G. Yuan, W. Jiang, B. Huang and Y. Sun, *Org. Electron.*, 2014, **15**, 1678.

29 B. Chen, J. Ding, L. Wang, X. Jing and F. Wang, *Chem. Commun.*, 2012, **48**, 8970.

30 M. Yu, S. Wang, S. Shao, J. Ding, L. Wang, X. Jing and F. Wang, *J. Mater. Chem. C.*, 2015, **3**, 861.

31 Z. Jiang, H. Yan, Z. Liu, C. Yang, C. Zhong, J. Qin, G. Yu and Y. Liu, *Org. Lett.*, 2009, **11**, 4132.

32 W. Hung, L. Chi, W. Chen, Y. Chen, S. Chou and K. Wong, *J. Mater. Chem.*, 2010, **20**, 10113.

33 J. Ye, C. Zheng, X. Ou, X. Zhang, M. Fung, C. Lee, *Adv. Mater.*, 2012, **24**, 3410.

34 C. Han, Z. Zhang, H. Xu, G. Xie, J. Li, Y. Zhao, Z. Deng, S. Liu and P. Yan, *Chem.-Eur. J.*, 2013, **19**, 141.

35 H. Sasabe, N. Toyota, H. Nakanishi, T. Ishizaka, Y. J. Pu and J. Kido, *Adv. Mater.*, 2012, **24**, 3212.

36 K. S. Yook, S. E. Jang, S. O. Jeon and J. Y. Lee, *Adv. Mater.*, 2010, **22**, 4479.

37 W. Jiang, H. G. Xu, X. X. Ban, G. L. Yuan, Y. M. Sun, B. Huang, L. Duan and Y. Qiu, *Org. Lett.*, 2014, **16**, 1140-1143.

38 P.-I. Shih, C.-H. Chien, F.-I. Wu and C.-F. Shu, *Adv. Funct. Mater.*, 2007, **17**, 3514.

39 C.-H. Wu, P.-I. Shih, C.-F. Shu and Y. Chi, *Appl. Phys. Lett.*, 2008, **92**, 233303.

40 Z. Jiang, Y. Chen, C. Yang, Y. Cao, Y. Tao, J. Qin and D. Ma, *Org. Lett.*, 2009, **11**, 1503.

41 C. Fan, Y. Chen, Z. Jiang, C. Yang, C. Zhong, J. Qin and D. Ma, *J. Mater. Chem.*, 2010, **20**, 3232

42 S. Sumalekshmy and K. R. Gopidas, *J. Phys. Chem. B.*, 2004, **108**, 3705.

43 T. Yu, P. Zhang, Y. Zhao, H. Zhang, J. Meng and D. Fan, *Org. Electron.*, 2009, **10**, 653.

44 H. J. Bollink, E. Barea, R. D. Costa, E. Coronado, S. Sudhakar, C. Zhen and A. Sellinger. *Org. Electron.*, 2008, **9**, 155.

45 Z. Zhang, W. Jiang, X. Ban, M. Yang, S. Ye, B. Huang and Y. Sun, *RSC. Adv.*, 2015, **5**, 29708.

46 J. Y. Li, T. Zhang, Y. J. Liang and R. X. Yang, *Adv. Funct. Mater.*, 2013, **23**, 619.

47 Z. Ge, T. Hayakawa, S. Ando, M. Ueda, T. Akiike, H. Miyamoto, T. Kajita and M. Kakimoto, *Adv. Funct. Mater.*, 2008, **18**, 584.